

# Solid-state dynamic processes in complex systems analyzed by two-dimensional isotropic–anisotropic correlation nuclear magnetic resonance

L. Frydman<sup>a)</sup> and S. Vallabhaneni

Department of Chemistry (M/C 111), University of Illinois at Chicago, Chicago, Illinois 60607-7061

Y. K. Lee

Graduate Group in Biophysics, University of California and Chemical Biodynamics Division, Lawrence Berkeley Laboratory, Berkeley, California 94720

L. Emsley

Département de la Recherche Fondamentale sur la Matière Condensée, Centre de Etudes Nucléaires de Grenoble, 38041 Grenoble, France

(Received 26 January 1994; accepted 23 March 1994)

We describe the application of a recently developed two-dimensional nuclear magnetic resonance (2D NMR) technique, variable-angle correlation spectroscopy, to the analysis of molecular motions in complex unlabeled solids. This technique separates the broad anisotropic chemical shift line shapes of nuclei in a sample according to the isotropic shift of each site. It can therefore be used to characterize molecular reorientations by monitoring the changes that these processes introduce in the resolved powder patterns as a function of temperature. Using the  $^{13}\text{C}$  NMR anisotropies of dimethylsulfone as a test case, we explored the potential applications of following such an approach. It was found that in contrast to what happens in nonexchanging systems, the anisotropic line shapes resolved by the variable-angle technique on an exchanging solid are different from line shapes that at similar temperatures can be recorded from a nonrotating sample. An explanation for these differences is presented, and the complete theory required to extract kinetic and geometric information from the experimental 2D line shapes is introduced and illustrated with computer simulations. The capability of this approach to analyze motions in complex systems is further demonstrated with a natural-abundance  $^{13}\text{C}$  variable-temperature NMR analysis of *L*-tyrosine ethyl ester; a reorienting compound possessing up to 11 inequivalent carbon sites in the solid phase.

## I. INTRODUCTION

In contrast to what happens in solution-state NMR, where the chemical shifts of individual sites are an exclusive function of their average electronic environments, peak positions in solid-state NMR spectra also depend on the relative orientation of a nuclear site with respect to the external magnetic field.<sup>1</sup> This dependence gives rise to the well-known spin-1/2 chemical shift anisotropy (CSA) powder patterns, resulting from the superposition of NMR signals arising from all possible orientations present in a polycrystalline or amorphous solid sample.<sup>2</sup> These line shapes offer a valuable tool for detecting and characterizing the presence of molecular reorientations in a solid.<sup>3,4</sup> Indeed, dynamic processes will introduce time variations in the resonance frequencies of the exchanging chemical sites, that can in turn affect the fine structure observed in a powder pattern.<sup>5</sup> The changes which occur in these spectra as a function of reorientational rates are reminiscent of the behavior observed in dynamic solution NMR;<sup>6</sup> the time scale of the solid-state NMR experiments being determined by the chemical shift separation due to the effects of the anisotropy between different orientations related by the dynamic process. Thus, when motional rates are much smaller than the frequency breadth of the CSA, spec-

tral line shapes carry little kinetic information. As the magnitude of the CSA and of the exchange rates become comparable however, in the so-called intermediate exchange regime, a series of significant line shape distortions occur from which both kinetic as well as mechanistic information about the nature of the motion can be determined.

In spite of its recognized usefulness and simplicity, the application of this type of line shape analysis to the evaluation of dynamic processes in solids has remained relatively uncommon.<sup>4,7–11</sup> This is in sharp contrast with other experiments involving chemical shift analyses of spin-1/2 nuclei, such as magic-angle spinning (MAS) NMR,<sup>12</sup> which have achieved a much more widespread acceptance.<sup>13</sup> Problems in the application of CSA-based analyses are not completely surprising when considering that broad anisotropic line shapes usually exceed the isotropic chemical shift differences among inequivalent sites. Then, as the number of different resonances increases, static line shape experiments rapidly lose most of their chemical resolution as well as the possibility of yielding clearly resolved changes in the individual powder patterns. These facts have confined dynamic CSA analyses to the study of either chemically simple or isotopically enriched systems; in most cases however, the technique is usually at a spectroscopic and/or synthetic disadvantage with respect to analogous proton or deuterium NMR approaches.<sup>14,15</sup>

Complications due to extensive peak overlap could be

<sup>a)</sup>Author to whom correspondence should be addressed. Camille and Henry Dreyfus New Faculty Awardee (1992–1997).

avoided if one were to monitor the powder pattern variations introduced by dynamics from CSA line shapes that are resolved according to the isotropic shifts of individual chemical sites. It is possible to achieve such separation by relying on 2D NMR techniques; i.e., by implementing an experiment where the broad powder patterns carrying the motional information for each site in the molecule appear separated along a second isotropic high-resolution frequency dimension. Different approaches have been proposed for obtaining this kind of spectra.<sup>16-24</sup> Most of them involve the acquisition of a bidimensional data set as a function of two time variables; a time  $t_a$  encoding the effects of the anisotropic chemical shifts, and a time  $t_i$  encoding the evolution due to the isotropic interactions. We have recently proposed an alternative technique to achieve this goal.<sup>22,25</sup> It involves the acquisition of time-domain data arising from a macroscopically rotating solid-state spin system as a function of a single acquisition time  $t$ , using the angle  $\beta$  of sample rotation with respect to the external magnetic field as a second spectroscopic variable. The phase  $\phi$  accumulated by nuclear magnetizations in such an experiment can then be written as

$$\phi(\beta, t) = \omega_i \cdot t + \omega_a(\theta, \phi) \cdot P_2(\cos \beta) t, \quad (1)$$

where  $\omega_i$  and  $\omega_a(\theta, \phi)$  are the isotropic and anisotropic frequencies of the spins in different crystallites, and

$$P_2(\cos \beta) = (3 \cos^2 \beta - 1)/2 \quad (2)$$

is the second-order Legendre polynomial of  $\cos \beta$ . Changing the spinning axis  $\beta$  scales the relative contribution of the anisotropic components to the total evolution undergone by each spin. Isotropic and anisotropic chemical shifts can therefore be correlated by Fourier analysis of the variable-angle spinning data set  $S(\beta, t)$ , regarded as an implicit function of the "extraction vector"  $[t, P_2(\cos \beta)t]$ :

$$I(\omega_i, \omega_a) = \int \int S(\beta, t) \exp\{-i[\omega_i \cdot t + \omega_a \cdot P_2(\cos \beta)t]\} dt d[P_2(\cos \beta)t]. \quad (3)$$

We have discussed elsewhere in detail convenient ways of evaluating this integral.<sup>22</sup> Figure 1 illustrates the type of spectrum that the resulting variable-angle correlation spectroscopy (VACSY) approach yields for a solid sample, using powdered hexamethylbenzene as an example. By selecting from these 2D  $^{13}\text{C}$  NMR spectra slices at the isotropic shifts  $\omega_i$  of the different sites, the full anisotropic line shapes that would arise from a static sample can easily be extracted.

Both from a sensitivity as well as from an experimental point of view, VACSY appears as a robust technique for extracting static-like powder patterns from multisite systems. We decided therefore to explore the potential applications of the technique to dynamic CSA analyses of motional processes in solids; the present study reports on the results of such investigations. We found that in contrast to what is observed in the case of nonexchanging solids, the anisotropic line shapes that VACSY affords when an exchange process in the intermediate regime is involved are different from those arising under similar conditions from a nonspinning powdered sample. This discrepancy is originated by the mecha-

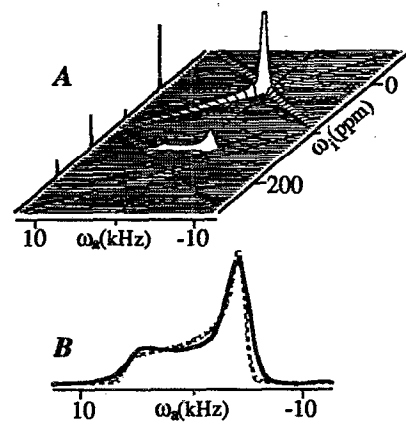


FIG. 1. (A) 2D VACSY isotropic-anisotropic  $^{13}\text{C}$  NMR correlation spectrum of hexamethylbenzene. The 1D trace on the left shows the projection along the isotropic axis, referenced to  $\delta_{\text{TMS}} = 0$  ppm. Thirty-one time-domain signals were acquired as a function of the spinning angle  $\beta$  for  $-0.5 \leq P_2(\cos \beta) \leq 0.5$ , and interpolated over a  $256 \times 64$  data points grid before Fourier transformation. The two tallest peaks correspond to the methyl- and quaternary-carbon resonances; the remaining peaks are spinning sidebands. (B) Comparison between the powder line shape extracted at the isotropic frequency of the aromatic carbons (continuous line), and a CSA pattern simulated using the single-crystal parameters reported for the site at room temperature (dashed line) (Ref. 26).

nism involved in the VACSY procedure; nevertheless, we show that when all due considerations are taken into account, experimental VACSY results cannot only be successfully rationalized but also used to extract kinetic and geometric information about molecular dynamics over a wide range of exchange rates.

## II. EXPERIMENT

Chemical samples employed throughout the present work were purchased from Aldrich; they all possessed a natural isotopic abundance and were used without further purification.  $^{13}\text{C}$  NMR experiments were carried out on a home-built spectrometer at a Larmor frequency of 75.78 MHz, and in all cases involved the use of standard  $^{13}\text{C}$  cross-polarization techniques from protons.<sup>27</sup> Samples were spun in 7 mm Doty Sci. rotors at rates of 3–5 kHz using a spinning assembly installed in a double-resonance single-coil home-made probehead. This system is equipped with a Whedco Inc. stepping motor that, commanded by the spectrometer pulse programmer, controls the angle  $\beta$  that the axes of both the sample spinning and the irradiation/observation coil subtend with the external magnetic field.<sup>28</sup> High-power decoupling fields are essential for retrieving undistorted CSA line shapes from protonated solids reorienting in the intermediate exchange regime.<sup>29</sup> Harman–Hahn matching conditions were therefore achieved using over 300 W in both the transmitter and decoupler channels, corresponding to proton nutation rates ranging between 93 and 55 kHz (depending on the angle of sample spinning).

The probehead achieves variable-temperature operation by heating the supplies of both the bearing and drive gas lines to the desired temperature with a dual set of heater

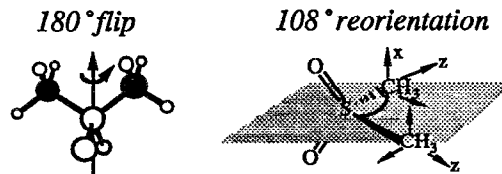


FIG. 2. Reorientations in solid DMS.  $180^\circ$  flips along the main molecular symmetry axis exchange the relative orientations of the carbon sites (filled circles, left) at temperature-dependent rates  $k = 5.44 \times 10^{13} \exp(-7601/T)$  Hz. These molecular motions result in mutual  $108^\circ$  rotations of the  $^{13}\text{C}$  chemical shift tensors around their  $x$  axes, as illustrated by the scheme on the right.

coils. Dried air was used for the experiments performed above room temperature; precooled gaseous nitrogen was supplied for the low-temperature measurements. Gas temperatures were monitored by a low-noise stainless steel thermocouple placed at the entrance to the pressurized chamber of the spinning assembly, and were kept constant within less than  $1^\circ\text{C}$  throughout the 2D signal acquisitions using a home-built system based on an Omega Inc. proportional controller. Absolute temperatures inside the spinning rotor were calibrated vs the thermocouple reading by analyzing the line shape of an off-magic angle spinning sample and are considered accurate within  $\pm 1.5^\circ\text{C}$ ; details about this procedure will be reported elsewhere. NMR data were collected using a Tecmag Inc. signal acquisition system interfaced to a Macintosh Quadra computer. All the required post-acquisition processing and spectral simulations were carried out on the same computer using home-written *C*-language programs.

### III. RESULTS

#### A. VACSY line shapes in the intermediate exchange regime: A test study

In order to evaluate the potential usefulness of VACSY for investigating molecular motions we focused our attention on dimethylsulfone (DMS); a compound which since initially studied by Solum *et al.*<sup>10</sup> has served extensively as a model system for dynamic solid-state NMR analyses. DMS (Fig. 2) possesses two chemically equivalent carbon sites whose CSA pattern can be clearly discerned in a normal  $^{13}\text{C}$  static cross-polarization experiment. Upon increasing temperatures DMS molecules start to undergo  $180^\circ$  reorientations about their main symmetry axes; rotations which produce well-defined changes in the  $^{13}\text{C}$  NMR powder line shapes. From the latter both the kinetics and geometries involved have been accurately extracted, thus providing us with a model case of solid-state dynamics where all the parameters involved are known.

Figure 3 illustrates a series of 2D VACSY NMR spectra obtained on a sample of DMS as a function of temperature. All spectra show an isotropic dimension whose resolution remains similar to the one observed under MAS conditions, and a cross peak whose anisotropic line shape shows a marked temperature dependence. The simultaneous fulfillment of these two conditions ensures the potential application of this technique to the study of dynamic CSA line

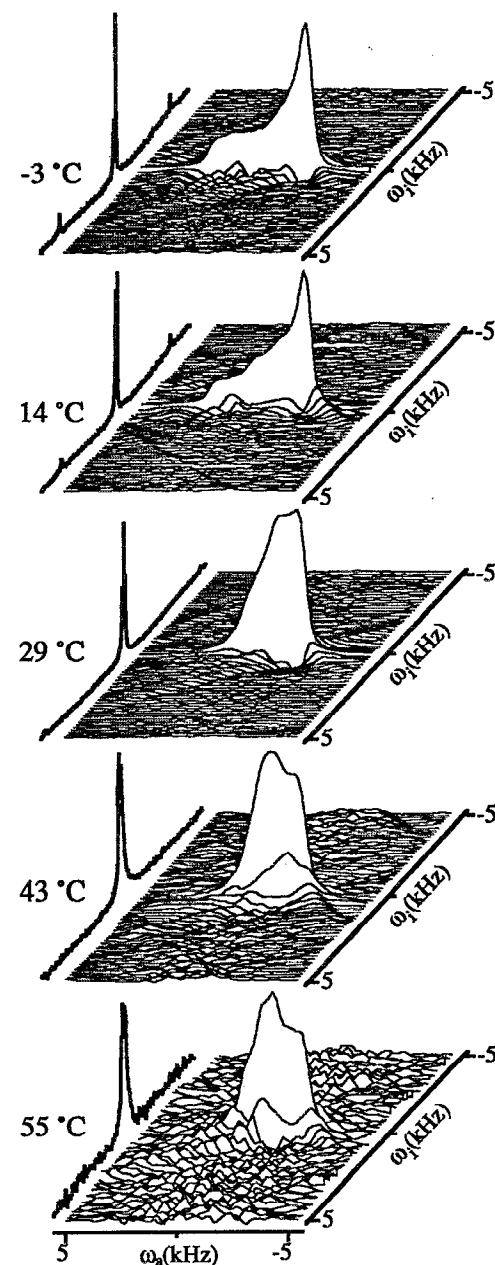


FIG. 3. 2D VACSY  $^{13}\text{C}$  NMR spectra (real part only) obtained on a DMS powder sample as a function of temperatures. Time-domain data were recorded using 31 spinning angles distributed over a  $-0.5 \leq P_2(\cos \beta) \leq 0.5$  range, chosen so as to afford equal spectral widths (10 kHz) along both frequency domains. Shown to the left of each 2D plot are the isotropic projections of the spectra; smaller peaks flanking the main resonances are spinning sidebands.

shapes in multisite systems. A close examination of the anisotropic line shapes that can be resolved from the 2D NMR spectra however, reveals that the well-defined singularities which develop in these DMS powder patterns as temperatures increase do not match the changes that are observed for a static sample at similar temperatures (Fig. 4). Moreover, the two experiments seem to be sensitive to different NMR time scales. At room temperature for instance the static

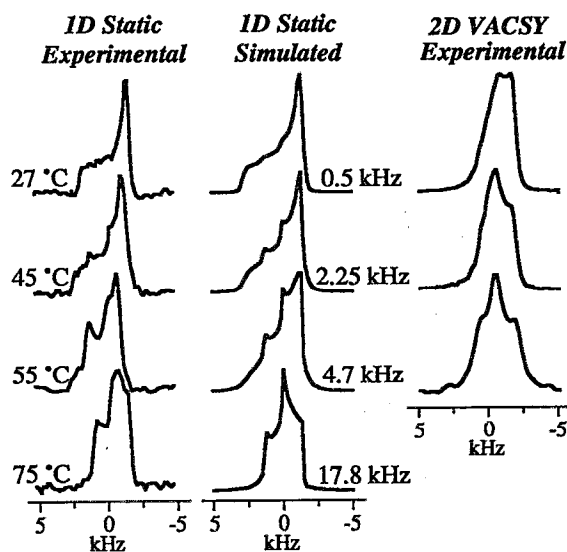


FIG. 4. Comparison between the experimental  $^{13}\text{C}$  NMR line shapes recorded on a static DMS sample as a function of temperatures (left-hand column), simulated distributions of the static experimental spectra calculated using the corresponding literature parameters (center column), and anisotropic slices that at similar temperatures can be extracted from the experimental 2D VACSY NMR spectra (right-hand column). Simulations were obtained from time-domain calculations as described in Ref. 3 using the geometric, kinetic, and chemical shift parameters reported by Solum *et al.* (Ref. 10). The exchange rates that were used are indicated to the right of each simulation; corresponding experimental temperatures are shown on the left. In all cases the frequency origin was placed at the center of mass of the powder line shapes.

sample still shows spectra with little evidence of molecular reorientations, whereas the VACSY patterns are already considerably distorted due to the effects of motions. On the other hand, the 2D experiment yields a motionally averaged pattern at temperatures ( $\sim 55$  °C) for which static line shapes are still well in the intermediate exchange regime.

It is possible to rationalize both time scale and line shape differences between static and VACSY results, by considering the ways in which motional processes interact with the operation of the latter technique. 2D VACSY NMR correlates isotropic and anisotropic chemical shifts by changing their relative contributions to the total time evolution undergone by spin coherences. These variations are achieved by selecting appropriate spinning axes  $\beta$ , which in turn scale all the anisotropies by equal factors  $P_2(\cos \beta)$  [see Eq. (1)]. As recently discussed by Schmidt and Vega however, these “scaling-only” considerations are no longer valid when molecular reorientations take place.<sup>30</sup> Since dynamic solid-state NMR line shapes depend on the ratio between the rate of reorientation to the width of the CSA, changing the effective frequency separation among exchanging sites by means of variable-angle spinning will also affect the overall time scale of the dynamic NMR experiment. Thus, even at constant rates of motion, powder patterns recorded at different angles of macroscopic spinning may reflect all regimes of dynamic solid-state NMR. An example of this kind of behavior is illustrated in Fig. 5, which shows how the variable-angle

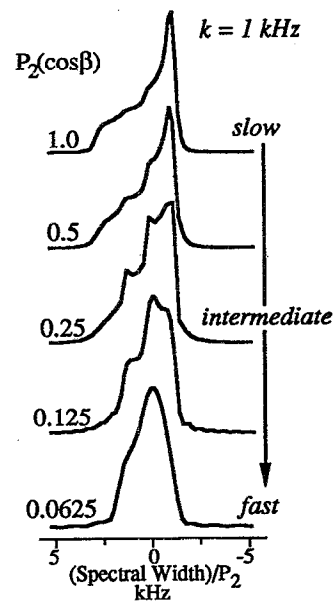


FIG. 5. Variations expected in the  $^{13}\text{C}$  chemical shift line shapes of fast-spinning DMS sample as a function of  $P_2(\cos \beta)$ . The plots were simulated assuming an exchange rate of 1 kHz ( $T \approx 33$  °C). The overall variable-angle spinning scaling is compensated by appropriate changes in the frequency axis; note however how CSA patterns evolve from slow- into intermediate- and on to fast-exchange regime line shapes as  $P_2(\cos \beta)$  approaches zero.

spinning line shapes of a site exchanging with the structural and kinetic parameters of DMS can be expected to change as a function of  $P_2(\cos \beta)$ . The final anisotropic line shapes appearing in 2D VACSY correlation spectra result from a weighted average of these distorted patterns; it is therefore not surprising that in the presence of dynamics the VACSY CSA line shapes depart from those observed for a static sample, showing an enhanced sensitivity towards slower motional reorientation rates when compared with the  $P_2(\cos \beta)=1$  static case.

In spite of these differences, anisotropic line shapes originating from 2D VACSY correlation experiments carry at least as much kinetic and geometric information as those available from static sample measurements. To extract such information however, it is necessary to take into account both the molecular details of the exchange process as well as the experimental angles of sample spinning involved in the 2D acquisition setup. Calculation of anisotropic VACSY line shapes can then proceed by simulation of the complete 2D variable-angle time-domain data set arising from the exchanging powder at a given rate, followed by the same bidimensional interpolation and Fourier processing that is applied on the experimental data. Slices extracted from such 2D simulated sets at the isotropic frequency of the site can be safely compared with the experimental dynamic CSA line shapes. We carried out this type of simulation on a system exchanging with structural and kinetic parameters identical to those reported for DMS; the rate-dependent anisotropic line shapes thus obtained show an excellent agreement with

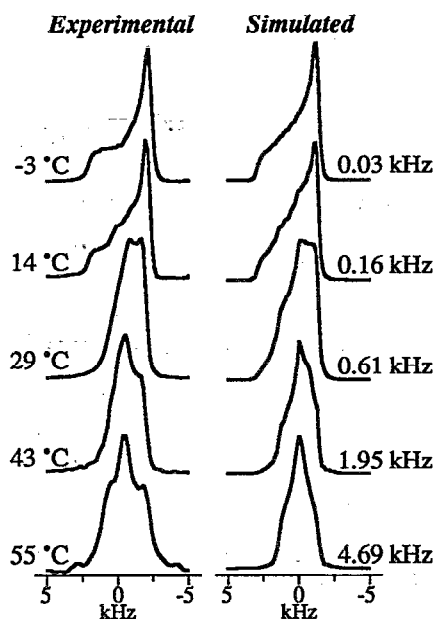


FIG. 6. Comparison between the experimental (left-hand column) and simulated (right-hand column) VACSY  $^{13}\text{C}$  anisotropic powder patterns of DMS. Experimental line shapes were extracted from the 2D distributions shown in Fig. 3. Simulated line shapes were calculated as described in the text using identical angular and processing parameters as those involved in the collection of experimental data; the exchange rates used in these simulations are shown to the right of each plot.

the experimental  $^{13}\text{C}$  VACSY patterns observed as a function of temperature (Fig. 6).

### B. Molecular dynamics in multisite systems: Tyrosine ethyl ester

An important advantage of using the 2D isotropic-anisotropic correlation technique for investigating molecular motions resides in its potential to analyze systems possessing several inequivalent chemical sites. To explore this aspect of natural-abundance  $^{13}\text{C}$  VACSY NMR we decided to investigate the dynamic process occurring in tyrosine ethyl ester. As initially noticed by Griffin and co-workers,<sup>31</sup> the  $^{13}\text{C}$  CP-MAS NMR spectra of this crystalline solid show a marked dependence on temperature. Whereas spectra recorded below 0 °C clearly exhibit one isotropic peak for each of the 11 inequivalent carbon sites in the molecule, a dynamic process makes the protonated phenyl carbons *ortho* to both the hydroxyl and the alkyl groups equivalent as temperature is increased (Fig. 7). The splittings observed at low temperature are characteristic of an -OH group whose fast rotation around the C–O bond is quenched in the solid. In crystalline compounds such as the one under consideration, where dynamic processes rarely disturb the translational symmetry of the lattice, the merging of peaks observed as temperature increases can originate either from the onset of 180° rotations of -OH groups around their C–O bonds, from synchronized H···O–H···O=H–O···H–O··· intermolecular hydrogen transfer processes, or from sudden 180° reorientations of the phenyl rings about their *para* axes. These three kinds of pro-

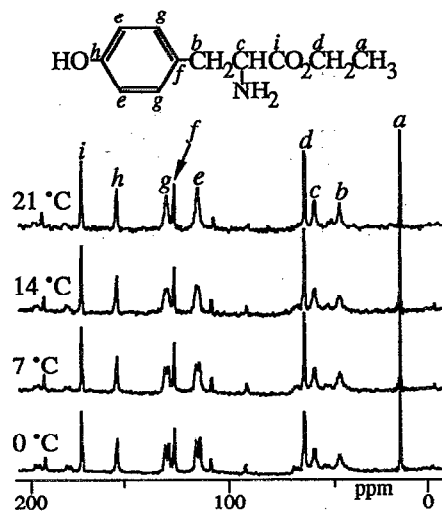


FIG. 7. Variable-temperature  $^{13}\text{C}$  CP-MAS NMR spectra of tyrosine ethyl ester, showing the thermally activated coalescence of the protonated aromatic carbon resonances. Assignments correspond to the positions indicated in the chemical structure shown on the top; unmarked resonances correspond to spinning sidebands.

cesses cannot be unambiguously distinguished by monitoring the changes in the isotropic  $^{13}\text{C}$  NMR chemical shifts of the molecule. The last type of dynamic behavior however, common in both crystalline and polymeric materials, can be discriminated from the others by measuring the variations taking place in the CSA parameters of the protonated aromatic carbons. Indeed, processes involving hydroxyl group dynamics will change the anisotropic shifts of these sites by an amount comparable to the splittings observed in the low-temperature MAS spectra (~3 ppm); phenyl ring reorientations on the other hand, will be associated with much larger changes (~50 ppm) arising from the mixing of the in-plane components of their CSA tensors. We therefore decided to further investigate the nature of the molecular motions occurring in tyrosine ethyl ester, by analyzing the changes observed in the isotropically resolved powder patterns of these carbons as a function of temperature.

A 2D VACSY  $^{13}\text{C}$  NMR spectrum recorded on the ester at low temperature is shown in Fig. 8; a listing of the corresponding CSA parameters is presented in Table I. In order to disregard possible interferences from peak *f* attention was focused on peak *e*, the clearly resolved signal arising from the carbons *ortho* to the methoxy group. For these sites, the CSA VACSY line shapes illustrated on the left-hand column of Fig. 9 were obtained as a function of temperature. The averaging observed among the least shielded components of the chemical shift tensor as temperature increases is diagnostic of 180° ring flip rotations; a possibility which we further explored by comparing the experimental VACSY results with the simulated line shapes which can be expected for this kind of motion. To carry out these simulations the principal shielding components available from experimental low-temperature  $^{13}\text{C}$  anisotropic line shapes were used. Following single-crystal and theoretical guidelines we placed the most shielded component of this tensor (*z* axis) perpendicu-

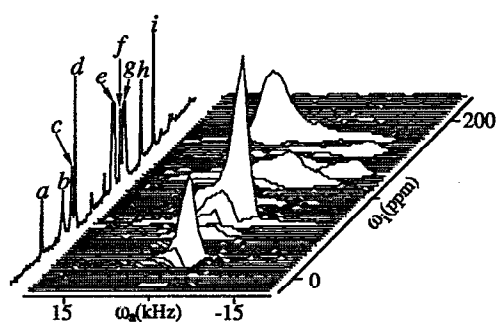


FIG. 8. 2D isotropic-anisotropic  $^{13}\text{C}$  NMR correlation spectrum of tyrosine ethyl ester at 0 °C. 256 data points were acquired in 31 time-domain experiments for spinning axes  $\beta$  spanning the range  $-0.25 \leq P_2(\cos \beta) \leq 0.25$ , and interpolated over a  $256 \times 64$  time-domain grid. The sampling setup that was used afforded an isotropic spectral width of 25 kHz and an anisotropic window of 50 kHz; the resulting digital resolution was not high enough to resolve the four signals observed in Fig. 7 for the protonated aromatic carbons. Peak assignments on the projection shown on the left correspond to the molecular structure shown in Fig. 7.

lar to the aromatic ring, and the least shielded direction (y axis) along the C–H bond (Fig. 9, top scheme). The effects of 180° ring flip motions were then taken into account by assuming mutual exchange processes between two classical sites whose CSA frequencies are related by 120° rotations of their tensors about the z axes. Complete dynamic VACSY time-domain simulations were carried out as described above, by integrating the signals arising from the exchanging sites over a solid sphere as a function of the macroscopic spinning angles  $\beta$  that were used to record the experimental data. Spectra calculated in this way using the appropriate rates of exchange (Fig. 9, right-hand column) reproduce the main features observed in the experimental temperature-dependent VACSY line shapes, thus lending support to the presence of ring-flip dynamic processes for tyrosine ethyl ester in the solid phase.

TABLE I.  $^{13}\text{C}$  NMR shielding parameters of L-tyrosine ethyl ester at 0 °C.<sup>a</sup>

Peak <sup>b</sup>	$\omega_i^c$	$\Delta\omega$ (ppm)	$\eta$
<i>a</i>	16.3	8	1.0
<i>b</i>	46.1	24	0.3
<i>c</i>	59.0	-15	0.2
<i>d</i>	64.2	-49	0.3
<i>e</i> <sup>d</sup>	116.7, 118.2	-91	0.7
<i>f</i>	129.0	-115	0.7
<i>g</i> <sup>d</sup>	132.1, 133.7	-125	0.5
<i>h</i>	157.9	-97	0.8
<i>i</i>	175.4	82.4	0.1

<sup>a</sup> Assuming  $|\omega_{33}| \geq |\omega_{22}| \geq |\omega_{11}|$ ;  $\omega_{11} + \omega_{22} + \omega_{33} = 0$ . Principal values are considered accurate within  $\pm 5$  ppm.

<sup>b</sup> Peak assignments are as shown in Fig. 7.

<sup>c</sup> Isotropic shifts reported downfield from  $\delta_{\text{TMS}} = 0$  in ppm, calibrated using hexamethylbenzene as an external reference.

<sup>d</sup> Not resolved in the 2D NMR spectrum due to insufficient digital resolution.

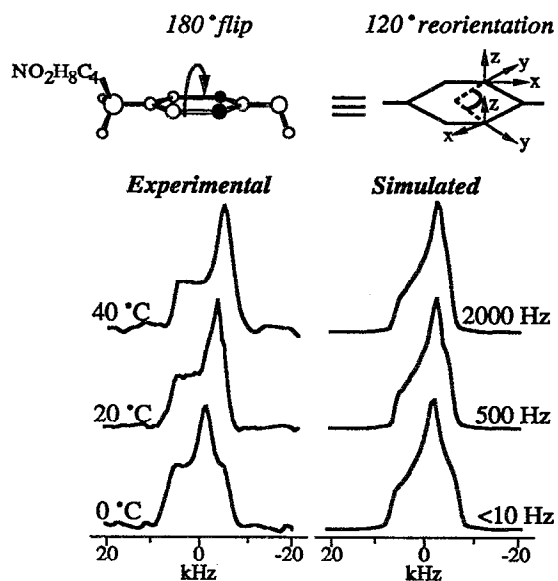


FIG. 9. Comparison between the experimental anisotropic line shape resolved for site *e* of tyrosine ethyl ester from variable-temperature VACSY spectra (left-hand column), and simulated distributions calculated assuming 180° flips of the aromatic rings taking place at the indicated rates (right-hand column). This reorientation brings about 120° rotations of the CSA tensors around their *z* axes as shown in the scheme on the top. Experimental spectra were recorded using the VACSY parameters described in Fig. 8. Simulations took into account these acquisition parameters as described in the text and the exchange rates shown on the right of each plot, chosen to fit the experimental data.

#### IV. DISCUSSION AND CONCLUSIONS

In spite of its sensitivity drawbacks, the remarkable capabilities of NMR for monitoring the orientation dependence of nuclear spin interactions have made from this technique one of the leading approaches for probing motional dynamics in solids. Nevertheless the combination of these capabilities with the other unique attribute of NMR, its power to resolve spectral peaks according to their chemical origin in a complex molecule, has remained an elusive goal. Widespread ways of achieving this kind of resolution have included the use of synthetic isotopic enrichment of a particular site with  $^{13}\text{C}$  or  $^{2}\text{H}$ ,<sup>11,15</sup> as well as the observation of second-order relaxation effects on molecular systems where first-order anisotropic shifts have been effectively averaged out.<sup>32,33</sup> The methodology discussed in the present study provides an alternative route to solve the conflict between the search for high chemical resolution and the maximization of the available anisotropic information, by separating these two contributions along two orthogonal frequency dimensions. Although such an approach requires slightly specialized hardware and the implementation of a bidimensional NMR experiment, its execution is relatively straightforward and readily compatible with both high sample spinning speeds and extreme temperatures operations. Extraction of dynamic information from VACSY line shapes requires time-domain simulations of complete 2D data sets; the methodology of these calculations however, follows directly from uni-

dimensional dynamic NMR formalisms which have been well-known and documented for years. Still, it would be interesting to investigate whether some of the alternative techniques developed for the 2D separation of anisotropic patterns can yield high-resolution dynamic information without suffering from such computational drawback.

An intrinsic disadvantage of all CSA-based analyses compared to, for instance, dynamic deuterium quadrupolar NMR, resides in the relative inaccuracy with which the interaction tensors can be oriented within molecular frames of reference. This may circumscribe the application of dynamic  $^{13}\text{C}$  line shape studies to cases similar to the ones described in the present work, where literature guidelines on chemical shift tensor orientations are highly reliable, or to systems where the complementary acquisition of isotropically resolved separated local field spectra is feasible.<sup>34</sup> Of course, the present technique compensates these disadvantages by being fully compatible with the analysis of complex unlabeled systems. We therefore trust that this type of isotropic-anisotropic 2D correlation techniques will help to extend the scope of applications of solid-state NMR to the study of different types of dynamic processes in materials.

## ACKNOWLEDGMENTS

We are grateful to Professor Alexander Pines (University of California, Berkeley) for his helpful suggestions and stimulating thoughts throughout this study. The instrumentation used in the present work was supported in part by the University of Illinois at Chicago. Acknowledgment is also made to the donors of the Petroleum Research Fund administered by the ACS, for partial support of this research (L. F.).

<sup>1</sup>A. Abragam, *The Principles of Nuclear Magnetism* (Oxford University, Oxford, 1985).

<sup>2</sup>N. Blomberg and T. J. Rowland, *Acta Metall.* **1**, 731 (1953).

<sup>3</sup>M. Mehring, *Principles of High Resolution NMR in Solids* (Springer, Berlin, 1983).

- <sup>4</sup>H. W. Spiess, *Dynamic NMR Spectroscopy* (Springer, Berlin, 1978).
- <sup>5</sup>S. Alexander, A. Baram, and Z. Luz, *Mol. Phys.* **27**, 441 (1974).
- <sup>6</sup>J. Sandström, *Dynamic NMR Spectroscopy* (Academic, New York, 1982).
- <sup>7</sup>M. D. Sevcik, J. Schaefer, and E. O. Stejskal, *ACS Symp. Ser.* **34**, 109 (1976).
- <sup>8</sup>D. E. Wemmer, D. J. Ruben, and A. Pines, *J. Am. Chem. Soc.* **103**, 28 (1981).
- <sup>9</sup>R. G. Griffin, *Methods Enzymol.* **72**, 108 (1981).
- <sup>10</sup>M. S. Solum, K. W. Zilm, J. Michl, and D. M. Grant, *J. Phys. Chem.* **87**, 2940 (1983).
- <sup>11</sup>A. K. Roy, A. A. Jones, and P. T. Inglefield, *Macromolecules* **19**, 1356 (1986).
- <sup>12</sup>J. Schaefer and E. O. Stejskal, *J. Am. Chem. Soc.* **98**, 1031 (1976).
- <sup>13</sup>C. A. Fyfe, *Solid State NMR for Chemists* (CFC, Guelph, 1983).
- <sup>14</sup>D. C. Look and I. J. Lowe, *J. Chem. Phys.* **44**, 2995 (1966).
- <sup>15</sup>H. W. Spiess, *Colloid. Polym. Sci.* **261**, 193 (1983).
- <sup>16</sup>E. Lipmaa, M. Alla, and T. Turherm, *Proceedings of the 19th Congress Ampere*, Heidelberg (1976, unpublished), p. 241.
- <sup>17</sup>Y. Yarim-Ägaev, P. N. Tutujian, and J. S. Waugh, *J. Magn. Reson.* **47**, 51 (1982).
- <sup>18</sup>A. Bax, N. M. Szeverenyi, and G. E. Maciel, *J. Magn. Reson.* **51**, 400 (1983).
- <sup>19</sup>A. Bax, M. Szeverenyi, and G. E. Maciel, *J. Magn. Reson.* **52**, 147 (1983).
- <sup>20</sup>R. C. Zeigler, R. A. Wind, and G. E. Maciel, *J. Magn. Reson.* **79**, 299 (1988).
- <sup>21</sup>R. Tycko, G. Dabbagh, and P. A. Mirau, *J. Magn. Reson.* **85**, 265 (1989).
- <sup>22</sup>L. Frydman, G. C. Chingas, Y. K. Lee, P. J. Grandinetti, M. A. Eastman, G. A. Barrall, and A. Pines, *J. Chem. Phys.* **97**, 4800 (1992).
- <sup>23</sup>Z. H. Gan, *J. Am. Chem. Soc.* **114**, 8307 (1992).
- <sup>24</sup>S. L. Gann, J. H. Baltisberger, and A. Pines, *Chem. Phys. Lett.* **210**, 405 (1993).
- <sup>25</sup>L. Frydman, G. C. Chingas, Y. K. Lee, P. J. Grandinetti, M. A. Eastman, G. A. Barrall, and A. Pines, *Isr. J. Chem.* **32**, 161 (1992).
- <sup>26</sup>A. Pausak, J. Tegenfeldt, and J. S. Waugh, *J. Chem. Phys.* **61**, 1338 (1974).
- <sup>27</sup>A. Pines, M. G. Gibby, and J. S. Waugh, *J. Chem. Phys.* **59**, 569 (1973).
- <sup>28</sup>M. A. Eastman, P. J. Grandinetti, Y. K. Lee, and A. Pines, *J. Magn. Reson.* **98**, 333 (1992).
- <sup>29</sup>L. Frydman and B. Frydman, *J. Chem. Phys.* **92**, 1620 (1990).
- <sup>30</sup>A. Schmidt and S. Vega, *Chem. Phys. Lett.* **157**, 539 (1989).
- <sup>31</sup>A. Schmidt, Ph.D. dissertation, The Weizmann Institute of Sciences, Rehovot, Israel (1989).
- <sup>32</sup>R. Voelkel, *Angew. Chem. Int. Ed. Engl.* **27**, 1468 (1988).
- <sup>33</sup>J. Schaefer and E. O. Stejskal, *Top. Carbon-13 NMR Spectrosc.* **3**, 283 (1979).
- <sup>34</sup>T. Nakai, J. Ashida, and T. Terao, *J. Chem. Phys.* **88**, 6049 (1988).